Electronic Supplementary Material (ESI) for Journal of Materials Chemistry A.
This journal is © The Royal Society of Chemistry 2016

Supporting Information

Click-Based Porous Cationic Polymer for Enhanced Carbon Dioxide Capture

Alessandro Dani*, Valentina Crocellà, Claudio Magistris, Valentina Santoro, Jiayin Yuan, Silvia Bordiga*.

Table of Contents

1 Materials 2
1.1 Synthesis of CB-PCP 1 2
1.2 Anion exchange on CB-PCP 1 2
1.3 CB-PCP Carbene synthesis 2
1.4 Synthesis of CB-PCP 1a 2
1.5 Synthesis of CB-PCP 1b 3
1.6 Synthesis of CB-PCP 1s 3
1.7 Modfied Debus-Radziszewski imidazolium synthesis mechanism 3
2 Techniques 3
2.1 Thermogravimetric analisys 3
2.2 N_2 and CO_2 adsorption measurements 4
2.3 SEM analisys 4
2.4 NMR 4
2.5 High resolution mass spectrometry 4
2.6 FTIR spectroscopy 4
2.7 Adsorption micro-calorimetry 4
2.8 C,H, N elemental analysis 5
3 Results 5
3.1 Elemental analysis 5
3.2 Dimer identification from the HR mass spectreometry 5
3.3 Trimer identification from the HR mass spectreometry 7
3.4 Tetramer identification from the HR mass spectreometry 8
3.5 MS^n Fragmentation of the pure dimer used to prove the chemical structure 10
3.6 MS^n Fragmentation of the dimer with one acetamide in order to prove the chemical structure 12
3.7 N_2 adsorption isotherms at 77K 12
3.8 Pore size distribution 13
3.9 SEM image 14
3.10 Thermogravimetric analysis 14
3.11 Carbon dioxide adsorption measurement 15
3.12 Micro-calorimetry 16

1 Materials

All solid and liquid starting materials were purchased from Sigma-Aldrich and used as received.

1.1 Synthesis of CB-PCP 1

The general procedure for the synthesis of CB-PCP, showed in Scheme 1 is the following: in the first vial tetrakis(4-aminophenyl)methane (0.228 g, 0.600 mmol) was dissolved in 16 mL of a solution of water:glacial acetic acid 50:50. In the second vial formaldehyde 37% solution in water (0.394 mL, 5.28 mmol) and methyl glyoxal 40% solution in water (0.812 mL, 5.28 mmol) were mixed with 2 mL of water and 1 mL of glacial acetic acid. The solutions of the two vials were mixed together and the solution immediately turned form transparent to dark yellow, the reaction ran for 12 hours at 80°C and the solution became dark brown. The polymer was purified by dialysis against MilliQ® water using the 3.5 kDa tubing, afterwards it was freeze-dried. The obtained CB-PCP material, named **1**, was in form of brown fine powder.

1.2 Anion exchange on CB-PCP 1

The general procedure for the anion exchange, represented in Scheme 1 is the following: the polymer solution, obtained as described before and prior to the dialysis, was mixed with 20 mL of a solution of sodium tetrafluoroborate ($NaBF_4$, 0.329 g, 3.00 mmol). The polymer immediately precipitate out form the solution, because the change of polarity induced from the anion exchange with more hydrophobic counterion, the precipitated polymer was gently agitated for 1 hour and then washed with water (3x20mL). The exchanged CB-PCP was then freeze-dried and the product, named **2**, is obtained in form of dark brown powder. The same procedure was followed for CB-PCP with other counterion using respectively a solution of: bis(trifluoromethane)sulfonimide lithium salt (Tf_2NLi, 0.758 g, 2.64 mmol); potassium hexaflorophosphate (KPF_6, 0.486 g, 2.64 mmol); and sodium trifluoromethanesulfonate (NaTfO, 0.454 g, 2.64 mmol). In all the cases, due to the hydrophobicity of the exchanged counterion, the polymer precipitate out from the solution. Samples were respectively named **3** (Tf_2N), **4** (PF_6^-), and **5** (TfO^-).

1.3 CB-PCP Carbene synthesis

CB-PCP **1** was used as starting material to introduce NHC carbene in the CB-PCP. The procedure, represented in Scheme 1c is the following: CB-PCP **1** (0.300 g) was hermetically sealed in a vial and flushed with N_2 in order to desorb the adsorbed moisture. In another hermetically sealed vial potassium tert-butoxide (0.250 g) was dissolved in 6 mL of anhydrous THF in N_2 atmosphere. The solution of potassium tert-butoxide was transferred inside the vial with CB-PCP **1** and stirred for 72 hours at room temperature. The formed CB-PCP NHC carbene, was washed with anhydrous THF (4x10mL), anhydrous methanol (4x10mL) and anhydrous dioxane (4x10mL). Every washing was performed in N_2 protected atmosphere in order to avoid the presence of moisture that can react with the NHC carbene deactivating it. The sample was then freeze-dried and the CB-PCP NHC carbene product, in form of bright brown fine powder was stored in glove box under N_2 atmosphere. The so obtained material was named **6**.

In order to investigate the effect of the concentration of the starting reagent on the final CB-PCP two samples were synthesized in more concentrated solutions.

1.4 Synthesis of CB-PCP 1a

The general procedure for the synthesis of CB-PCP **1a**, is similar to the one of sample **1**, except for the volume of the solution. In the first vial tetrakis(4-aminophenyl)methane (0.228 g, 0.600 mmol) was dissolved in 8 mL of a solution of water:glacial acetic acid 50:50. In the second vial formaldehyde 37% solution in water (0.394 mL, 5.28 mmol) and methyl glyoxal 40% solution in water (0.812 mL, 5.28 mmol) were mixed with 1 mL of water and 0.5 mL of glacial acetic acid. In this case, a gelation of the entire solution instantly occured forming a dark violet gel. Even though the reaction was immediate, the reaction ran for 12 hours at 80°C in a hermetically sealed vial, in order to obtain a better cross-linking of the network, since gelation process reduced the molecular motions. The gel was then washed with a water:glacial acetic acid 50:50 solution (3x20 mL), then pure water (3X20 mL), afterwards it was freeze-dried. The obtained CB-PCP material was in form of brown fine powder.

1.5 Synthesis of CB-PCP 1b

The general procedure for the synthesis of CB-PCP **1b**, is similar to the one of **1**, except for the volume of the solution. In the first vial tetrakis(4-aminophenyl)methane (0.228 g, 0.600 mmol) was dissolved in 4 mL of a

solution of water:glacial acetic acid 50:50. In the second vial formaldehyde 37% solution in water (0.394 mL, 5.28 mmol) and methyl glyoxal 40% solution in water (0.812 mL, 5.28 mmol) were mixed with 0.5 mL of water and 0.25 mL of glacial acetic acid. In this case, a gelation of the entire solution instantly occured forming a dark violet gel. Even though the reaction was immediate, the reaction ran for 12 hours at 80°C in a hermetically sealed vial, in order to obtain a better cross-linking of the network, since gelation process reduced the molecular motions. The gel was then washed with a water:glacial acetic acid 50:50 solution (3x20 mL), then pure water (3X20 mL), afterwards it was freeze-dried. The obtained CB-PCP material was in form of brown fine powder.

1.6 Synthesis of CB-PCP 1s

The procedure for the synthesis of CB-PCP **1s**, the linear polymer used in the HR-MS, is the following: in the first vial tetrakis(4-aminophenyl)methane (0.0114 g, 0.030 mmol) was dissolved in 0.8 mL of a solution of water:glacial acetic acid 50:50. In the second vial formaldehyde 37% solution in water (0.00462 mL, 0.030 mmol) and methyl glyoxal 40% solution in water (0.00223 mL, 0.030 mmol) were mixed with 0.2 mL of water and 0.1 mL of glacial acetic acid. The solutions of the two vials were mixed together and the solution immediately turned form transparent to dark yellow, the reaction ran for 12 hours at 80°C and the solution became dark brown. The solution so obtained was used for the flow injection analysis in the LTQ-Orbitrap® mass spectrometer.

1.7 Modfied Debus-Radziszewski imidazolium synthesis mechanism

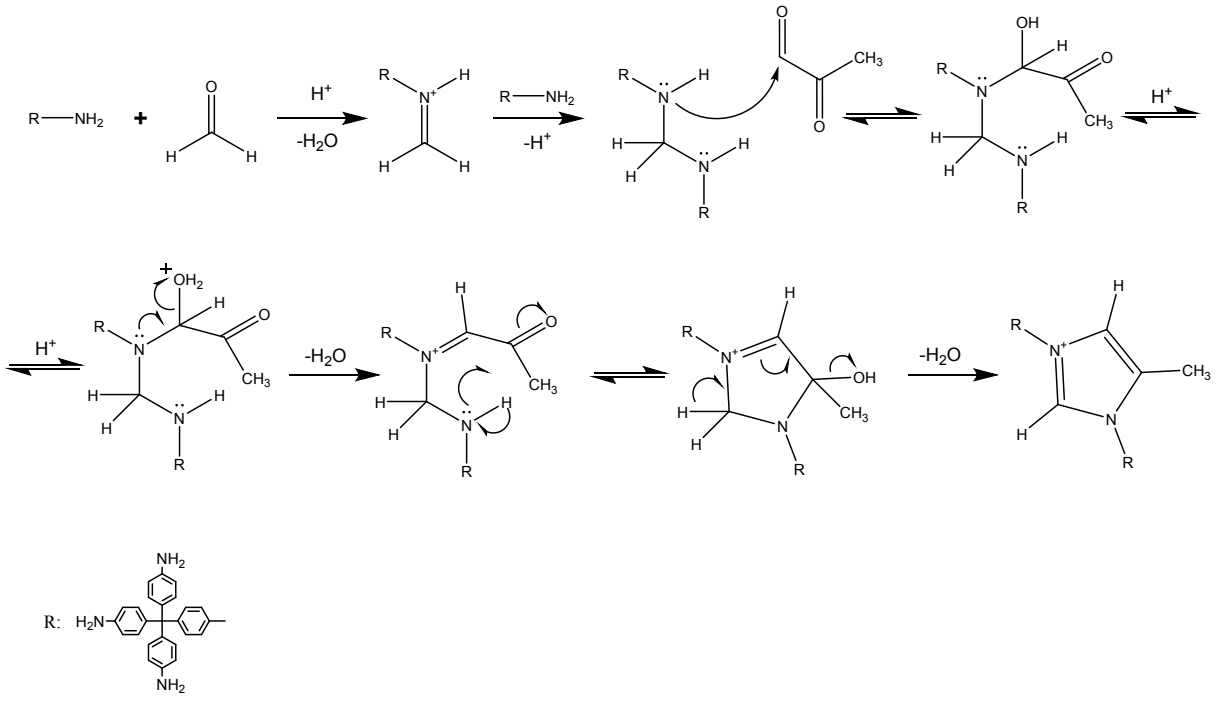

Figure S1. Proposed mechanism for imidazolium ring formation.

2 Techniques

2.1 Thermogravimetric analisys

TGA measurements were performed under N_2 flow in the range of 30–800˚C (ramp 2˚C min^{-1}) using an alumina pan, by means of a TA Q600 analyzer.

2.2 N_2 and CO_2 adsorption measurements

N_2 adsorption measurements at 77 K and CO_2 adsorption at different temperature were performed using Micromeritics ASAP2020. The samples were outgassed for 24 h at 353 K before all measurements. The surface area of the polymers was calculated by means of the BET algorithm and the Langmuir approximation in the standard p/p_0 range.

2.3 SEM analisys

The morphological properties of the polymers were studied using a SEM Zeiss EVO-50 XV, using a LaB6 source operating at 30 kV current in a high vacuum.

2.4 NMR

Solid state NMR (SS-NMR) spectra were acquired on a Bruker Avance III 500 spectrometer and a wide bore 11.7 Tesla magnet with operational frequencies for ^{1}H and ^{13}C of 500.13 and 125.77 MHz, respectively. A 4 mm triple resonance probe with MAS was employed in all the experiments. The samples were packed on a Zirconia rotor and spun at a MAS rate of 15 kHz. The relaxation delay, d1, between accumulations was between 8.5 s for ^{1}H MAS and ^{13}C CP-MAS NMR. For the $^{13}C\{^{1}H\}$ CP-MAS experiments, the radio frequency fields υ_{rfH} of 55 and 28 kHz were used for initial excitation and decoupling, respectively. During the CP period the ^{1}H RF field υ_{rfH} was ramped using 100 increments, whereas the ^{13}C RF field υ_{rfC} was maintained at a constant level. During the acquisition, the protons are decoupled from the carbons by using a TPPM (two pulse phase modulation) decoupling scheme. A moderate ramped RF field υ_{rfH} of 62 kHz was used for spin locking, while the carbon RF field υ_{rfC} was matched to obtain optimal signal and the CP contact time of 2 ms was used. All chemical shifts are reported using δ scale and are externally referenced to TMS at 0 ppm.

2.5 High resolution mass spectrometry

Sample CB-PCP **1s** was analyzed by means of LTQ-Orbitrap mass analyzer (Thermo Scientific, Rodano, Italy) equipped with an electrospray ionization source (ESI). The flow injection analysis was performed using a 1000 mg/L solution of Sample **1s** in methanol and a flux of 20µL/min. The analysis was performed in positive ion mode and the parameters of the ESI source were: 16V for capillary voltage and 55V for tube lens. The capillary, magnetic lenses, and collimating multi pole voltages were optimized, and the collision energy (CE) was generally chosen to maintain about 10% of the precursor ion. Mass accuracy was ± 5 ppm. All mass spectra were obtained with resolution of 30000 (500 m/z FWHM). Collision induced dissociation energy (CID) and precursor ion for MS^{n} analyses are written in the top-left part of each mass spectra.

2.6 FTIR spectroscopy

ATR-IR spectra were recorded on a Bruker Vertex 70 spectrophotometer equipped with a MCT detector. Each spectrum was recorded at a resolution of 2 cm^{-1} and 32 scans in the range of 4000–600 cm^{-1}.

In-situ FT-IR spectroscopy analysis was performed on a Bruker Vertex 70 spectrophotometer equipped with a MCT detector. Each spectrum was recorded at a resolution of 2 cm^{-1} and 32 scans in the range of 4000–600 cm^{-1}. Sample **6** were manipulated in glove box under N_2 atmosphere in order to avoid contact with moisture which can deactivate the carbene. The samples were dispersed in anhydrous methanol, deposited on an IR transparent silicon wafer and then the solvent was evaporated. The silicon wafer with the polymer deposition was then transferred into a special IR cell equipped with two KBr windows. This cell allows the manipulation of the sample in controlled atmosphere while collecting the FT-IR spectra. The cell was linked to a treatment line in order to outgas the sample until for 4 hours at room temperature until $1\cdot10^{-4}$ mbar of residual pressure. After the activation the sample was exposed to growing pressure of carbon dioxide from 0 to 200 mbar and leave in contact with CO_2 for 1 hour. At the end of the experiment the sample was outgassed until $1\cdot10^{-4}$ mbar of residual pressure. FT-IR spectra were recorded at each stages.

2.7 Adsorption micro-calorimetry

CO_2 heats of adsorption were measured, at 298 K, by means of a heatflow microcalorimeter (Calvet C80, Setaram, France) connected to a grease-free high-vacuum gas-volumetric glass apparatus (residual $p \approx 10^{-8}$ Torr) equipped with a Ceramicell 0-100 Torr gauge and a Ceramicell 0-1000 Torr gauge (by Varian), following a well established stepwise procedure. This procedure allows to determine, during the same experiment, both integral heats evolved ($-Q_{int}$) and adsorbed amounts (n_a) for very small increments of the adsorptive pressure. Before each measurement the samples, inserted in the calorimetric cell, were outgassed for one night at 353K until $1\cdot10^{-4}$ mbar. The cell was then inserted inside the calorimeter and equilibrated for one night at 298 K.

Adsorbed amounts have been plotted vs. pressure in the form of volumetric (quantitative). The adsorption heats observed for each small dose of gas admitted over the sample (q_{diff}) have been finally reported as a function of coverage, in order to obtain the (differential) enthalpy changes associated with the proceeding adsorption process. The differential-heat plots presented here were obtained by taking the middle point of the partial molar heats ($\Delta Q_{int}/\Delta n_a$, kJ/mol) vs na histogram relative to the individual adsorptive doses.

In all quantitative/calorimetric experiments, after the first adsorption run carried out on the bare activated samples (the primary isotherm), samples were outgassed overnight at the adsorption temperature (298 K), and

then a second adsorption run was performed (the secondary isotherm), in order to check whether secondary and primary adsorption runs coincided, or an irreversible adsorbed fraction was present.

2.8 *C,H, N elemental analysis*

Sample 1 was analyzed by Mikroanalytisches Laboratorium Kolbe Höhenweg 17, D-45470 Mülheim an der Ruhr.

3 Results

3.1 Elemental analysis

Table S1. Percentage of C, H, and N of sample **1**, obtained from two repetitions of elemental analysis. Calculated values are reported as reference.

entry	**% C**	**% H**	**% N**
calculated	74.98	5.30	9.20
sample **1**	74.78	5.55	9.11
sample **1** (repetition)	74.80	5.56	9.12

3.2 Dimer identification from the HR mass spectreometry

In the mass spectrum of Figure S1 the signals related to the dimer and to the dimer with various amides on the free amine are present. The amide formed through the reaction between the amine and the acetic acid present in the solvent. The amides moieties can form in any free amine and their distribution is statistically, based depending on the concentration of acetic acid in respect to the free amine. Table S1 reports the exact m/z ratio of the dimer and of the dimer with growing number of amides. All the molecules are evident in the mass spectra reported in Figure S1, except for the dimer with all the amino groups in form of amide, because this molecule is not statistically favoured at the used concentration of acetic acid in solution.

Table S2. Exact m/z ratio of the dimer, and of the dimer with growing number of amides.

number of acetamide	m/z
0	809.4075
1	851.4181
2	893.4286
3	935.4392
4	977.4498
5	1019.4603
6	1061.4709

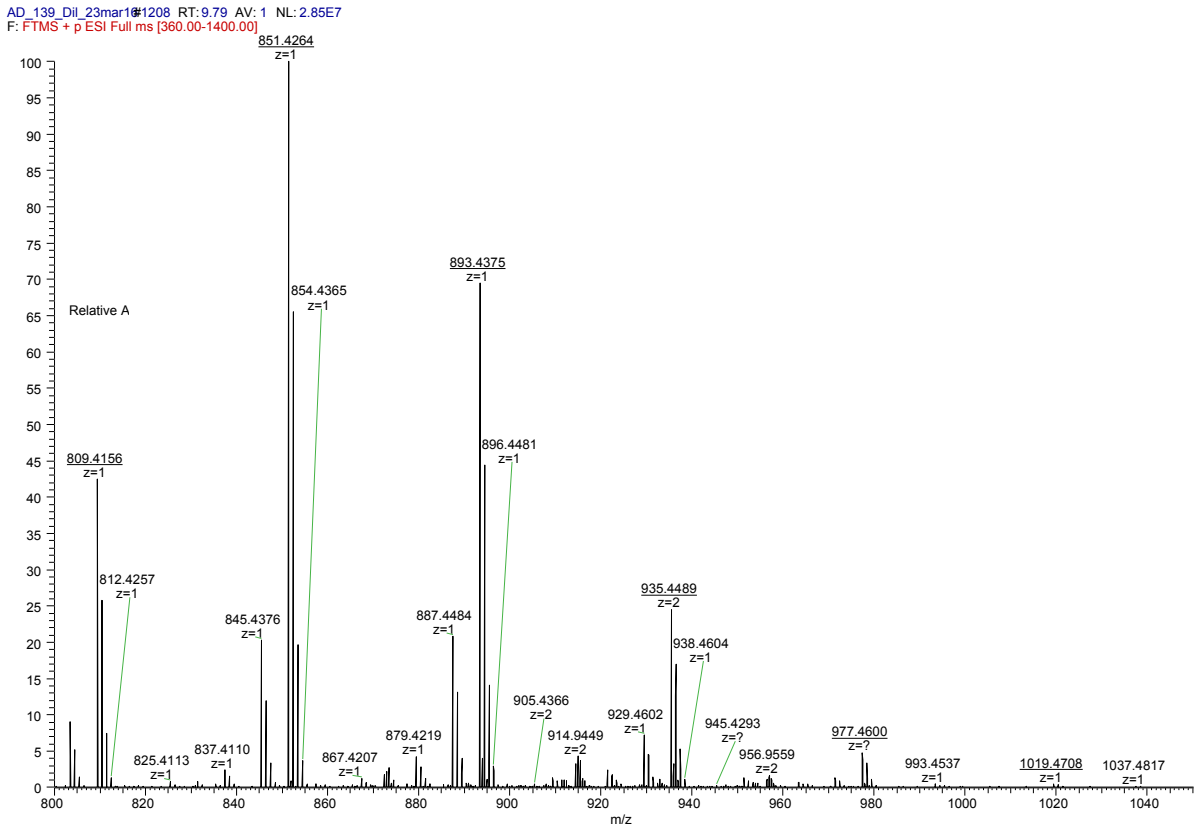

Figure S2. HR-Mass spectrum of sample **1s** in the 800-1050 m/z range. The underlined m/z refer to the tetramer in the various amide shapes.

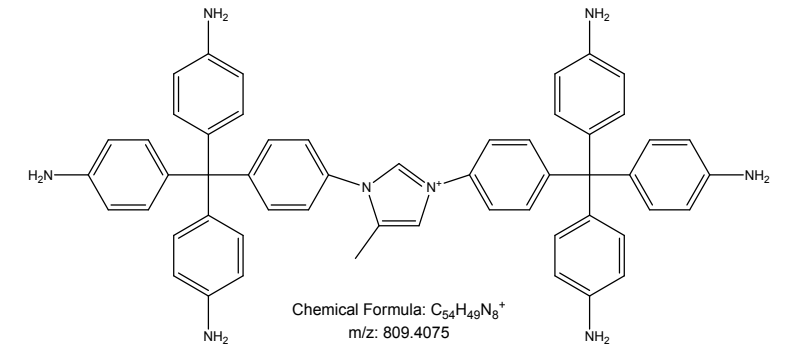

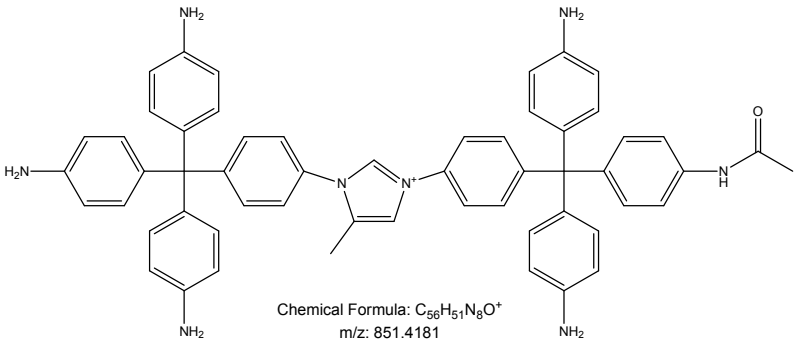

3.3 Trimer identification from the HR mass spectreometry

In the mass spectrum of Figure S2 the signals related to the trimer and to the trimer with various amides on the free amine are present. Table S2 reports the exact m/z ratio of the trimer and of the trimer with growing number of amides moiety. All the molecules are evident in the mass spectra reported in Figure S2, except for the trimer with seven and eight amino groups in form of amide, because these molecules are not statistically favoured at the used concentration of acetic acid in solution.

Table S3. Exact m/z ratio of the trimer, and of the trimer with growing number of amides.

number of acetamide	m/z
0	619.3074
1	640.3127
2	661.3180
3	682.3233
4	703.3286
5	724.8355
6	745.8408
7	766.8461
8	787.8514

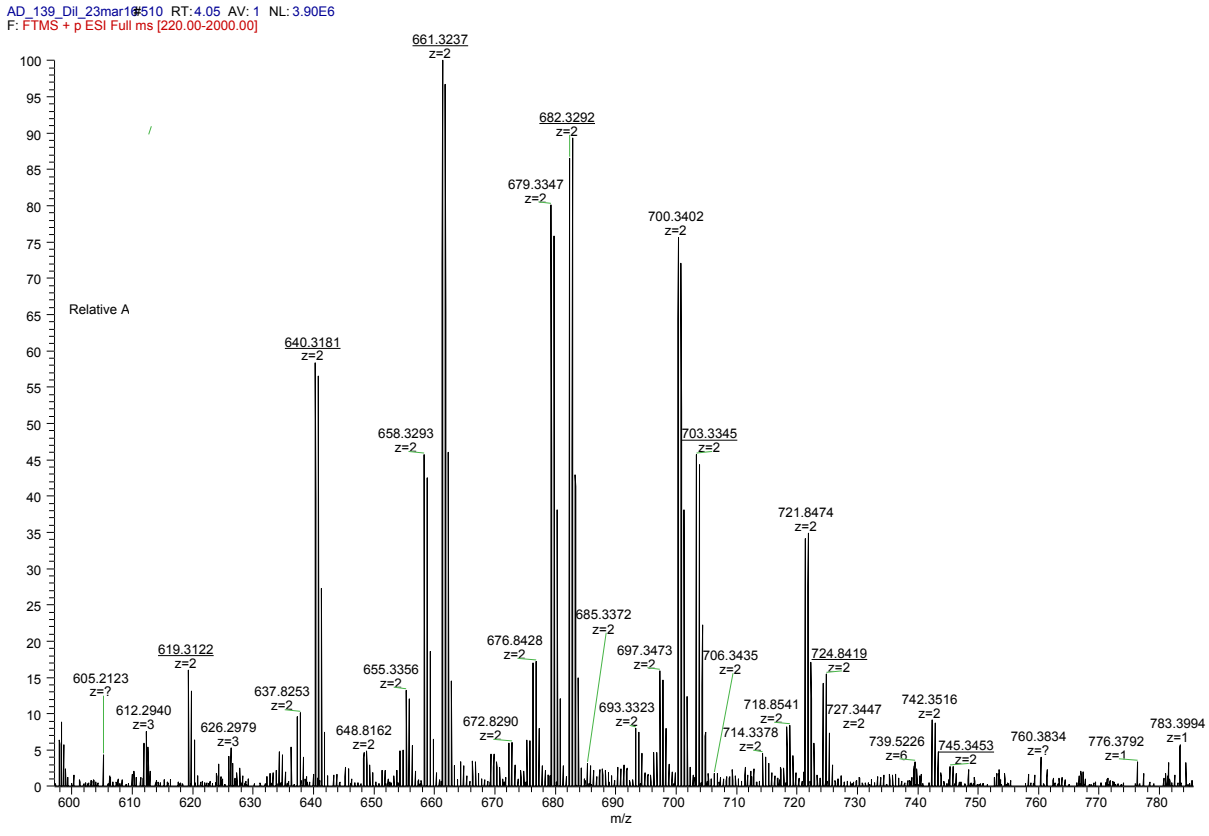

Figure S3. HR-Mass spectrum of sample **1s** in the 600-800 m/z range. The underlined m/z refer to the tetramer in the various amide shapes.

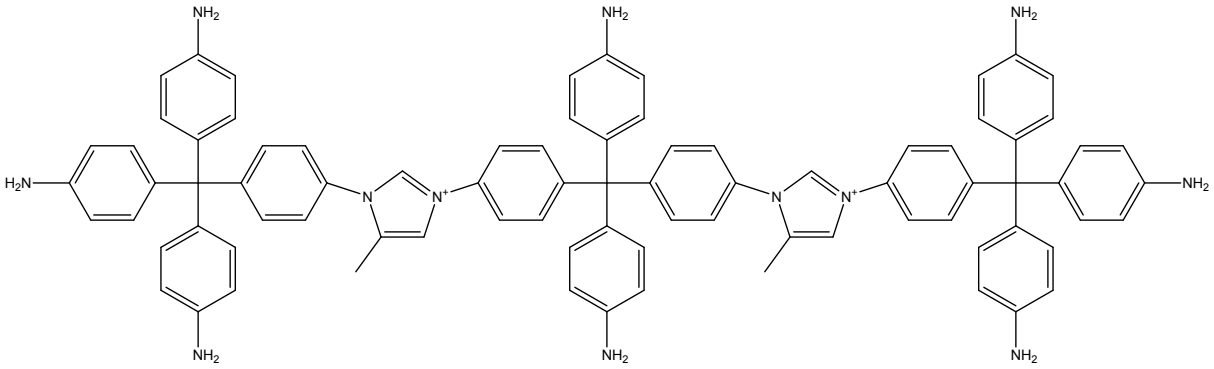

Chemical Formula: $C_{83}H_{74}N_{12}^{2+}$
m/z: 619.3074

3.4 Tetramer identification from the HR mass spectreometry

In the mass spectrum reported in Figure S3 the signals related to the tetramer and to the tetramer with various amides on the free amines are present. Table S3 reports the exact m/z ratio of the tetramer and of the tetramer with growing number of amides. The molecules evident in the mass spectra reported in Figure S3, are only the tetramers with one to five of the amino groups in form of amides, because only these molecules are statistically favoured at the used concentration of acetic acid in solution giving a signal high enough to be detected by the mass spectrometer.

Table S4. Exact m/z ratio of the tetramer, and of the tetramer with growing number of amides.

number of acetamide	m/z
0	556.2752
1	570.2787
2	584.2822
3	598.2858
4	612.2893
5	626.2928
6	640.2963
7	654.2999
8	668.3034
9	682.3096
10	696.3104

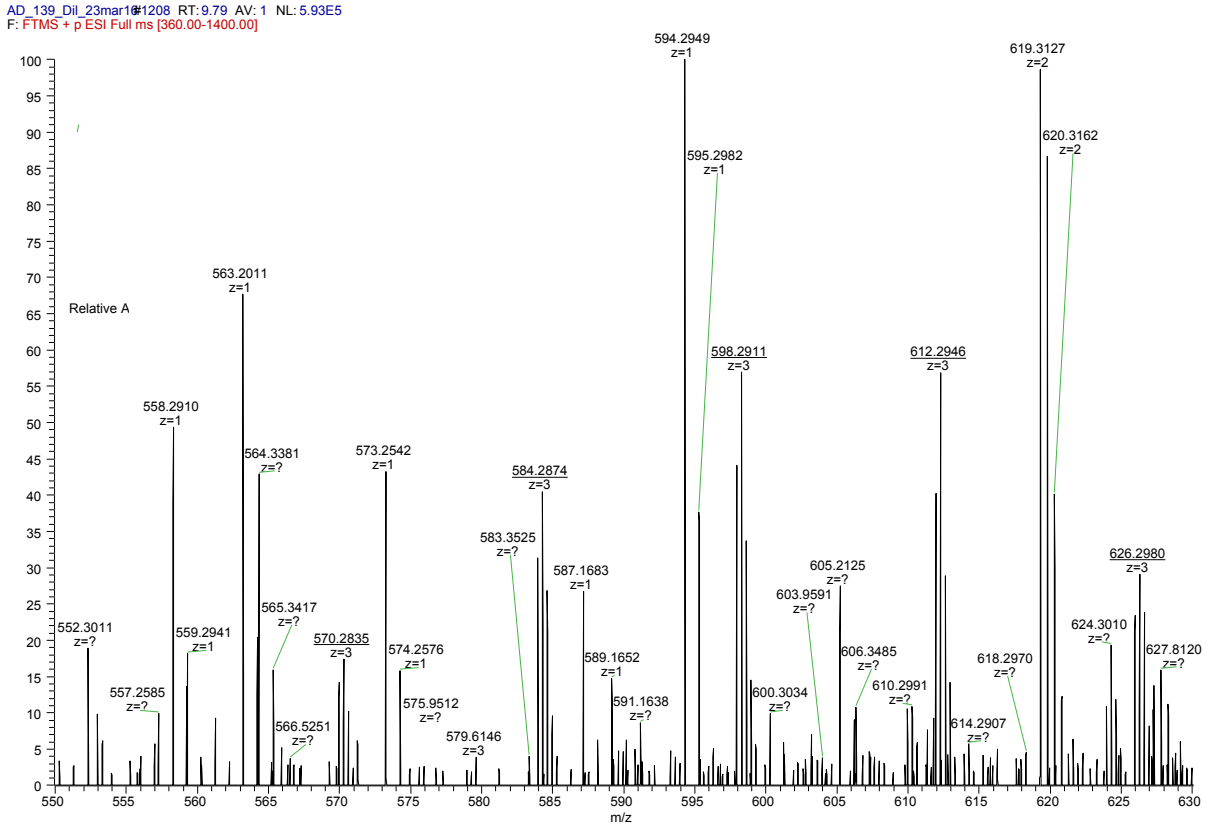

Figure S4. HR-Mass spectrum of sample **1s** in the 550-630 m/z range. The underlined m/z refer to the tetramer in the various amide shapes.

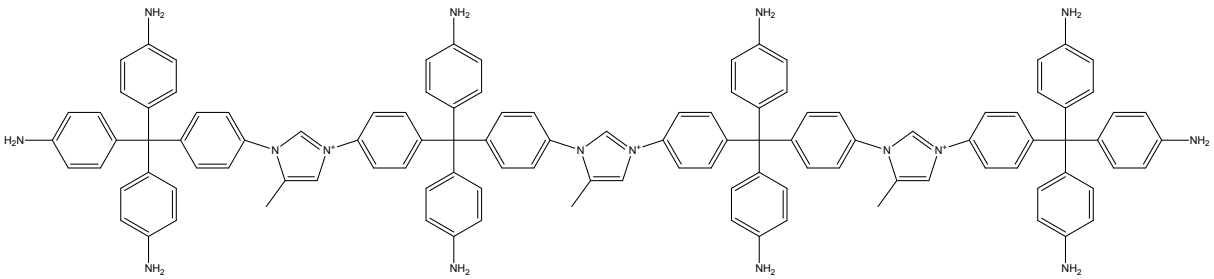

3.5 MS^n Fragmentation of the pure dimer used to prove the chemical structure

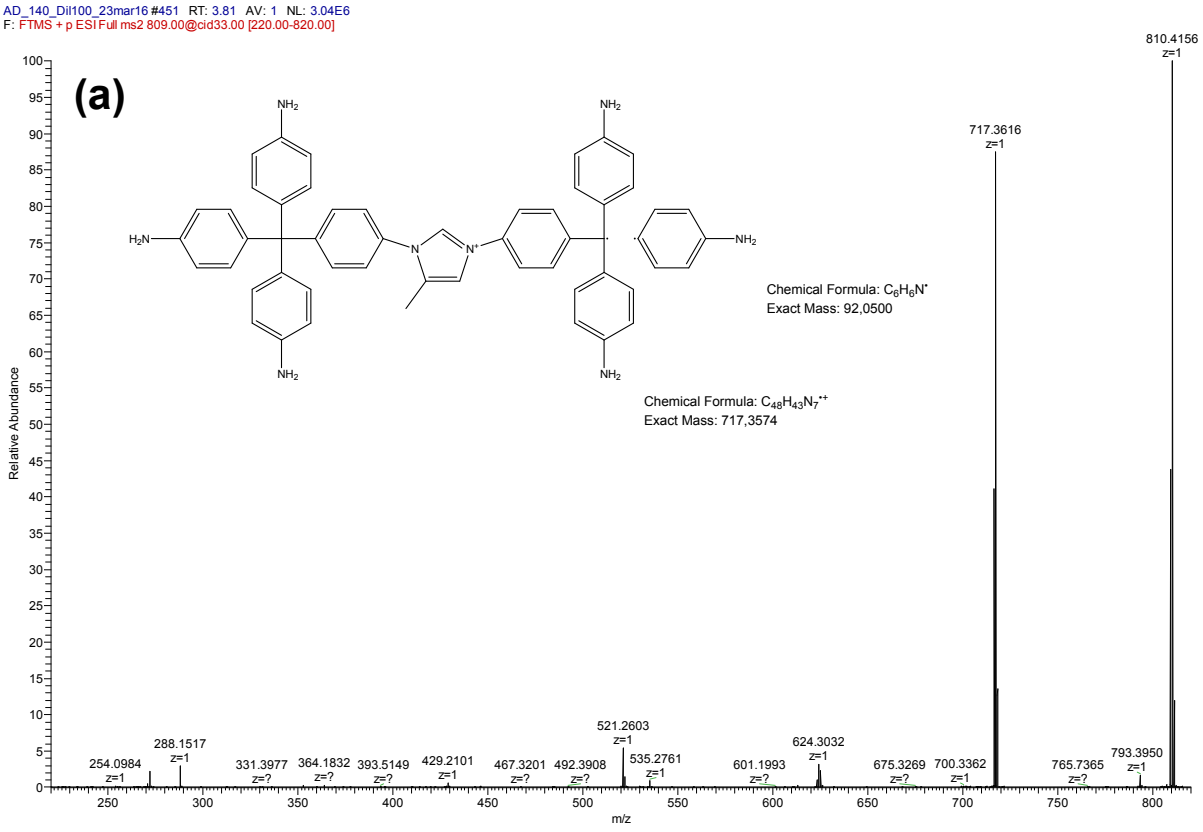

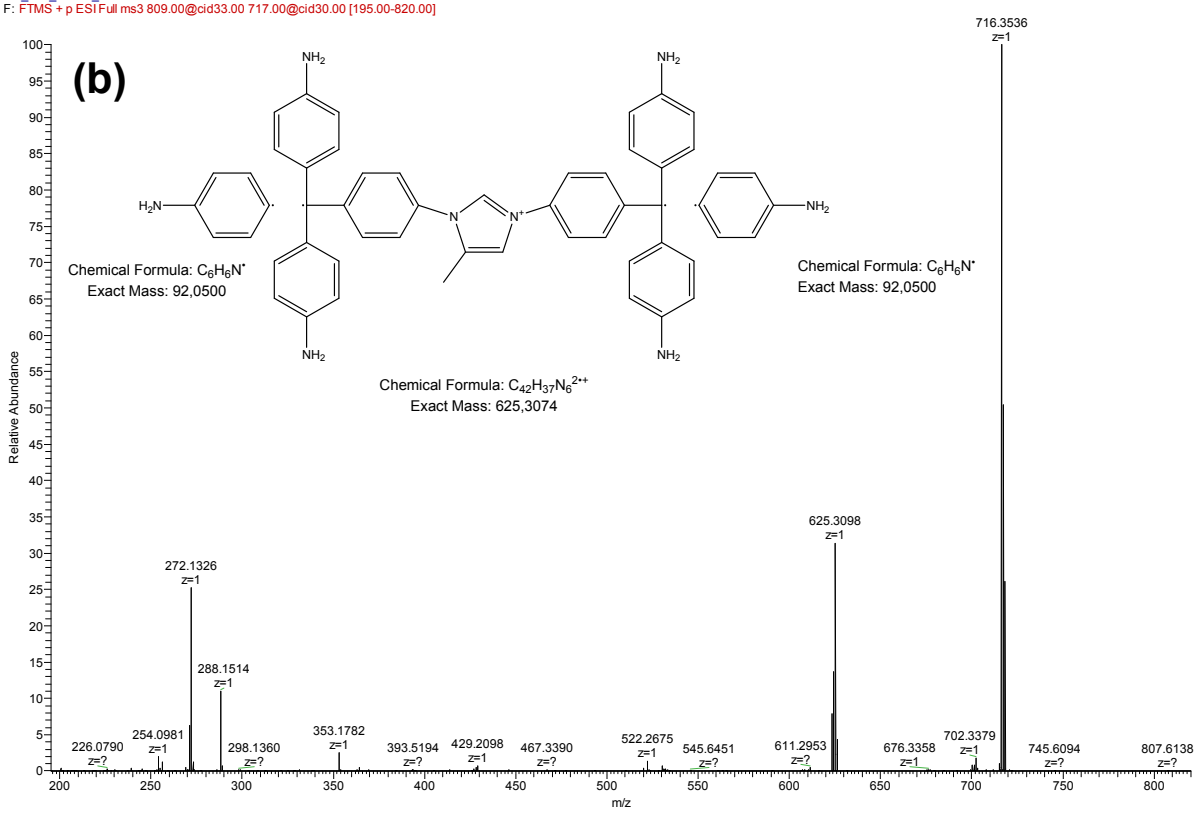

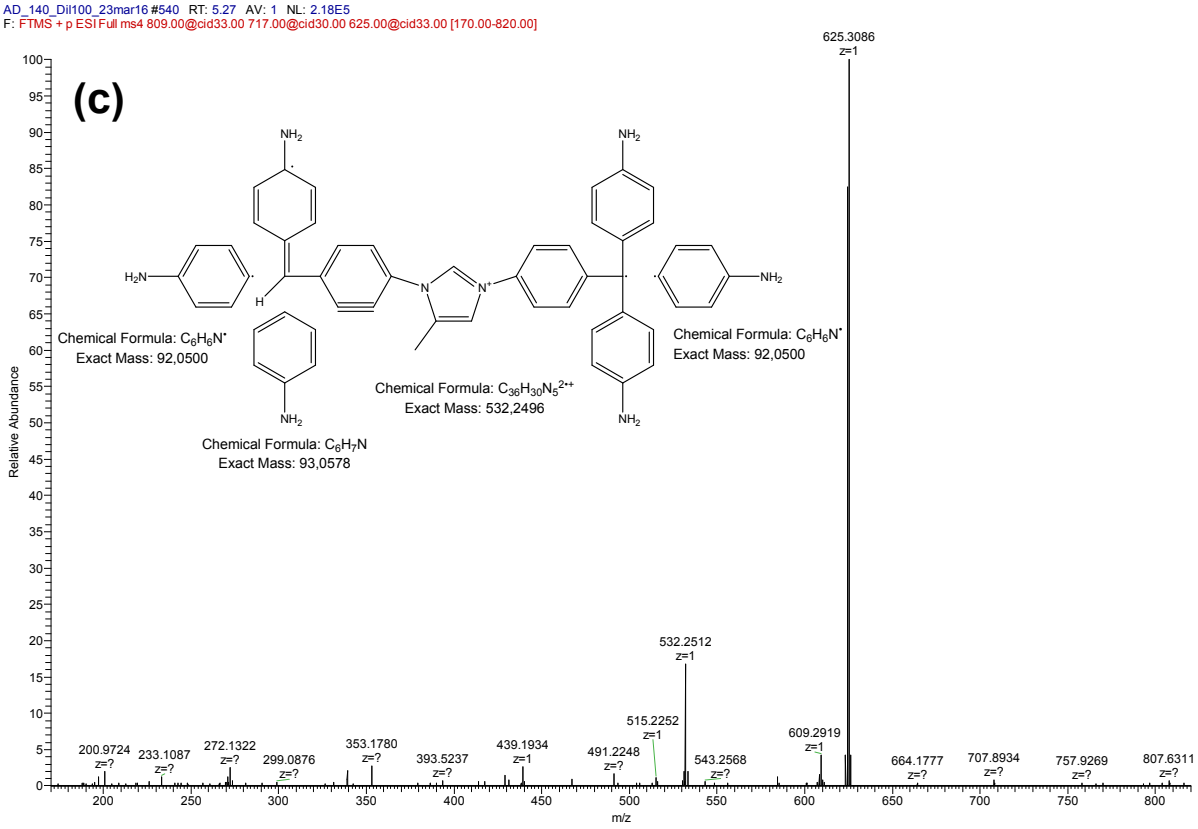

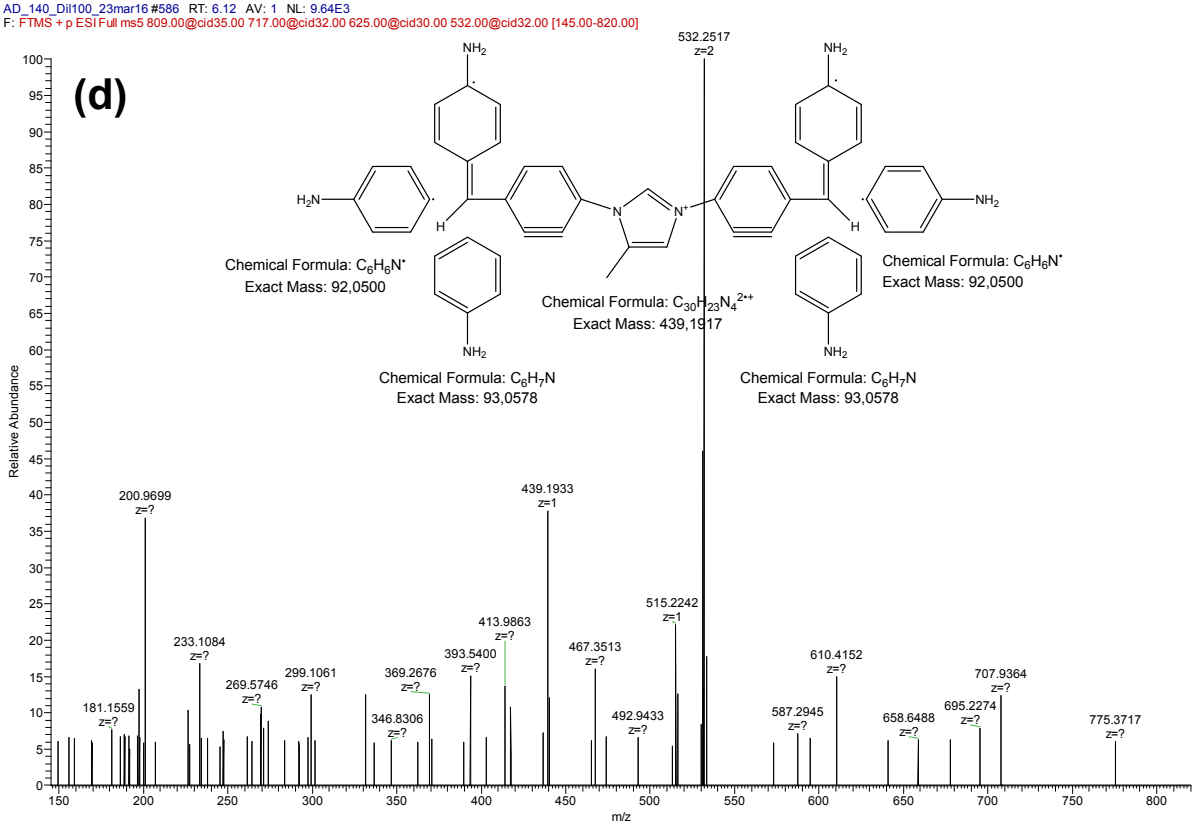

Figure S5. MS^n fragmentation of the dimer without amide moiety in the 150-800 m/z range. Part a refers to MS^2, part b to MS^3, part c to MS^4, part d to MS^5. Every MS spectrum has a proposed fragmentation scheme.

3.6 MS^n Fragmentation of the dimer with one acetamide in order to prove the chemical structure

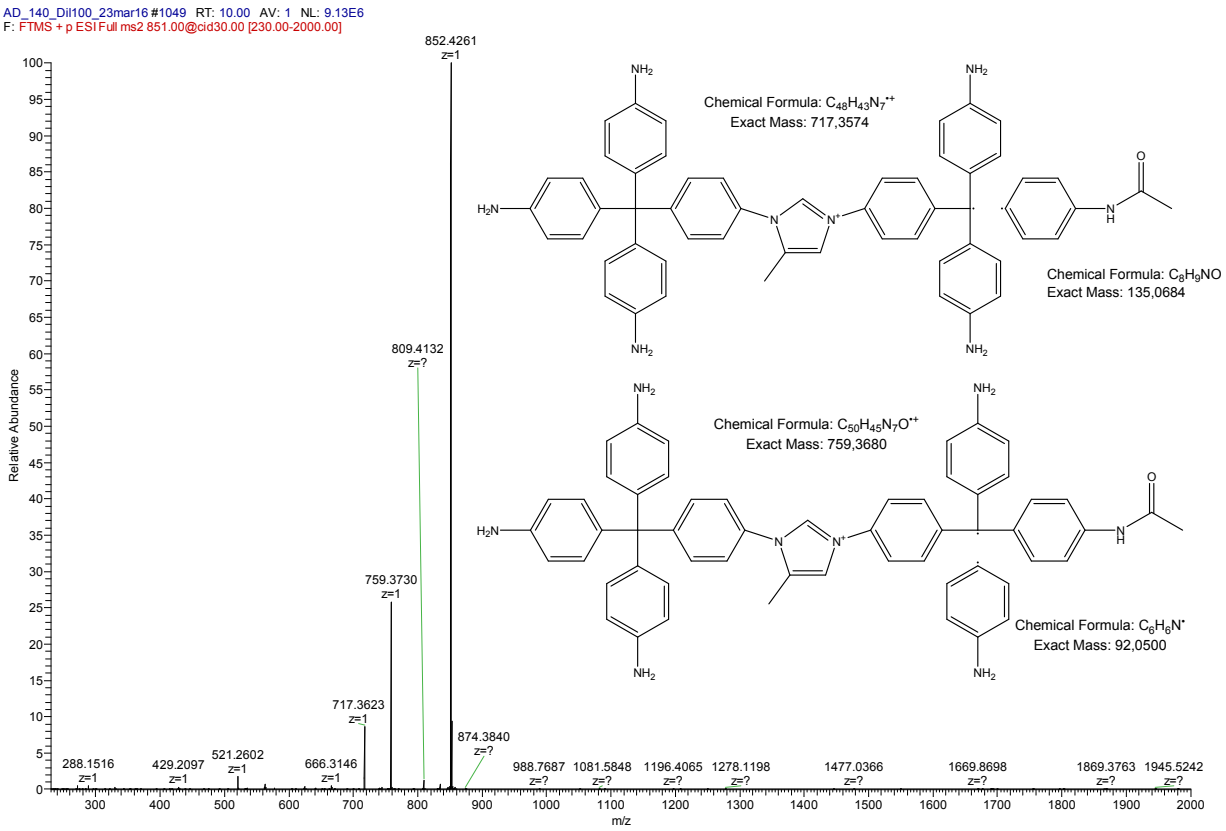

Figure S6. MS^2 fragmentation of the dimer with one amide in the 150-800 m/z range. Two fragmentation pathways occur together due to the neutral loss of unit with and without amide; both have a proposed fragmentation scheme.

3.7 N_2 adsorption isotherms at 77K

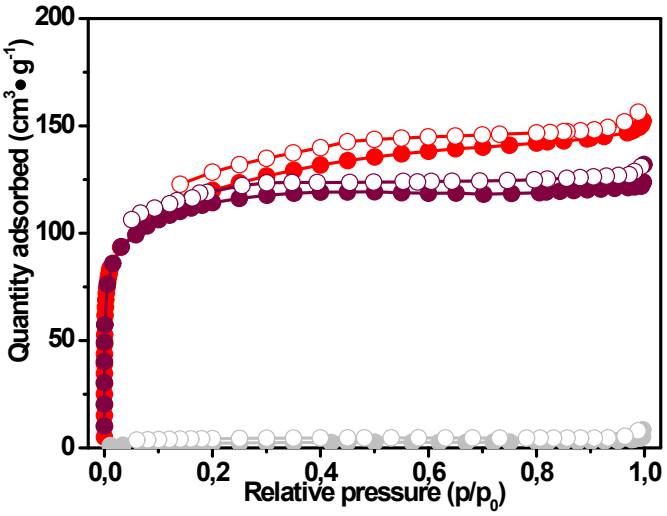

Figure S7. N_2 adsorption isotherms at 77K for samples: **1** (red curve), **1a** (rusty curve), **1b** (light gray curve).

3.8 Pore size distribution

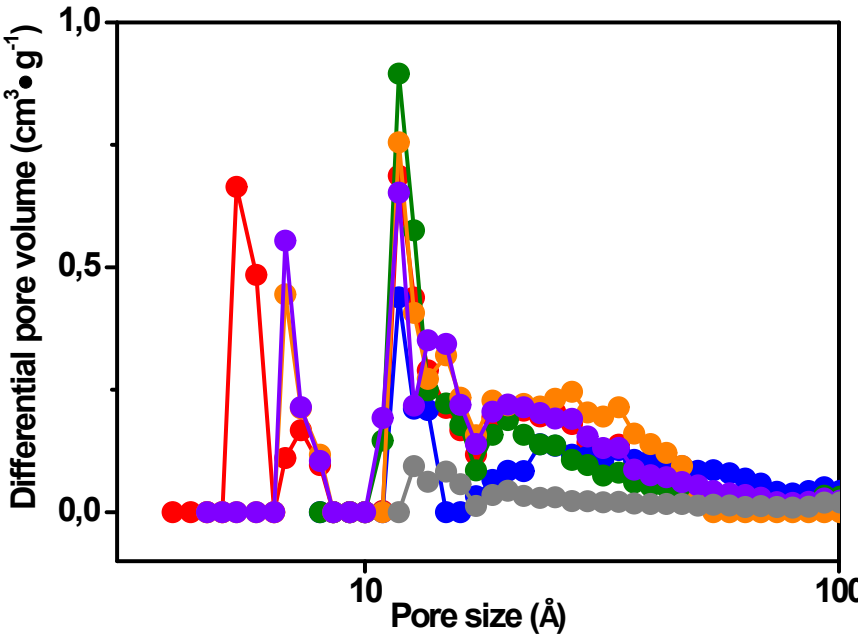

Figure S8. Pore size distribution obtained from the N_2 adsorption isotherms at 77K using non-local density functional theory (NL-DFT) and pore model for carbon with slit pore geometry. Results of the isotherms analysis are reported for samples: **1** (red curve), **2** (blue curve), **3** (green curve), **4** (orange curve), **5** (violet curve) and **6** (dark grey curve).

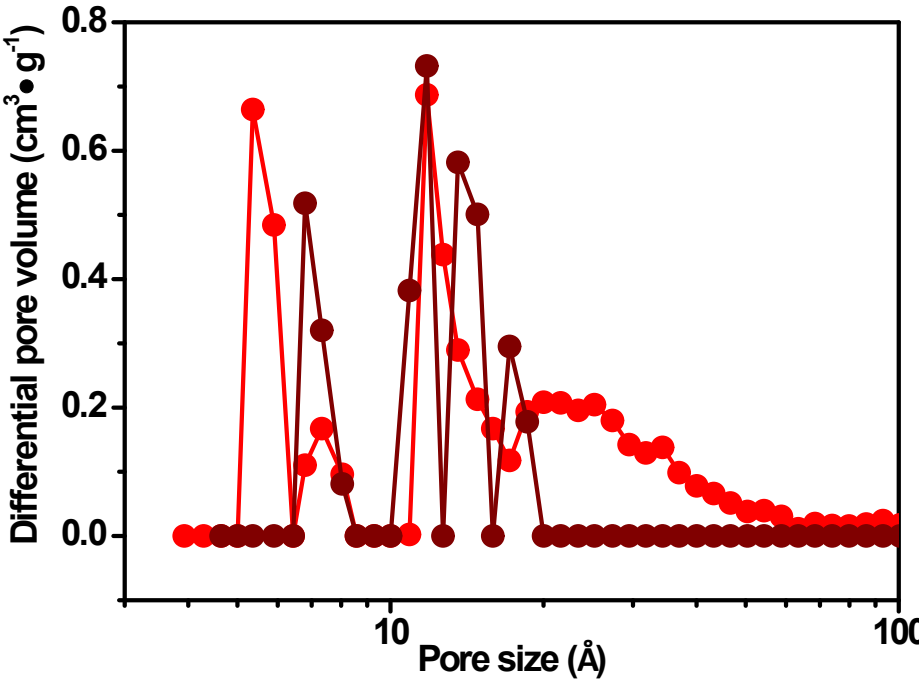

Figure S9. Pore size distribution obtained from the N_2 adsorption isotherms at 77K using non-local density functional theory (NL-DFT) and pore model for carbon with slit pore geometry. Results of the isotherms analysis are reported for samples: **1** (red curve), **1a** (rusty curve).

3.9 SEM image

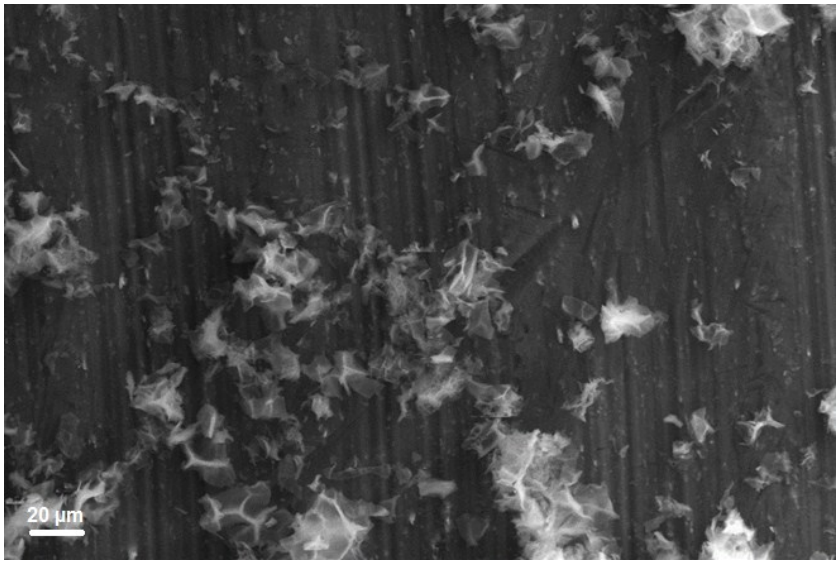

Figure S10. SEM picture of sample **1**

3.10 Thermogravimetric analysis

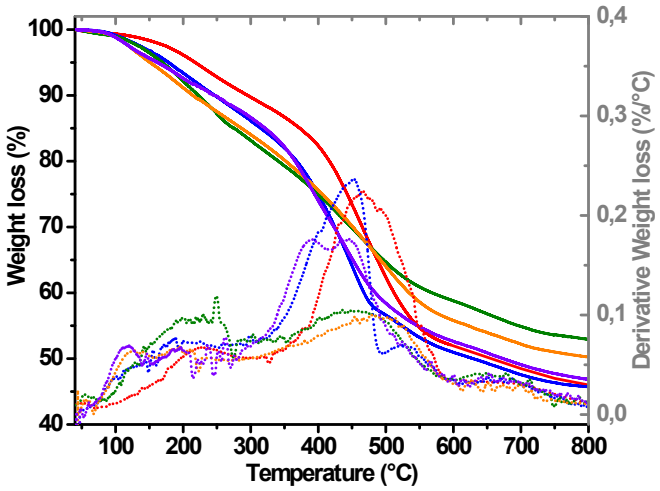

Figure S11. Thermogravimetric profiles (full curves) and derivative weight loss (dotted curves) for samples: **1** (red), **2** (blue), **3** (green), **4** (orange) and **5** (violet).

3.11 Carbon dioxide adsorption measurement

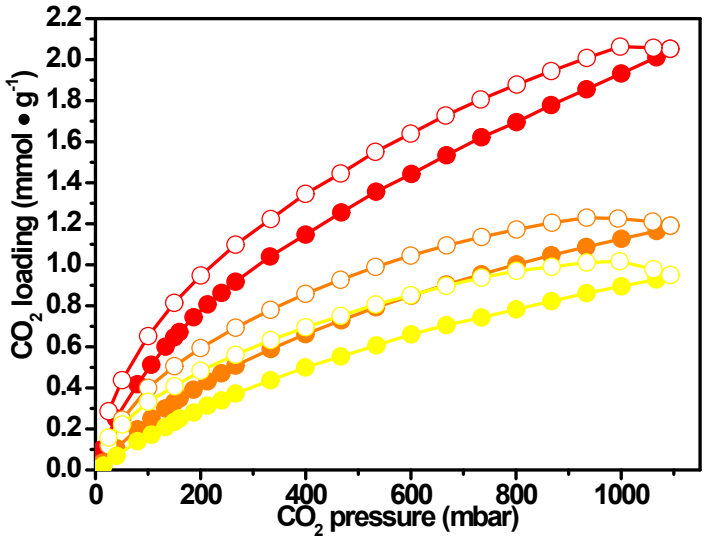

Figure S12. Carbon dioxide adsorption isotherm for samples **1** at: 273K (red curve), 298K (orange curve), 313K (yellow curve). Spheres and circles describe the adsorption branch and the desorption branch respectively.

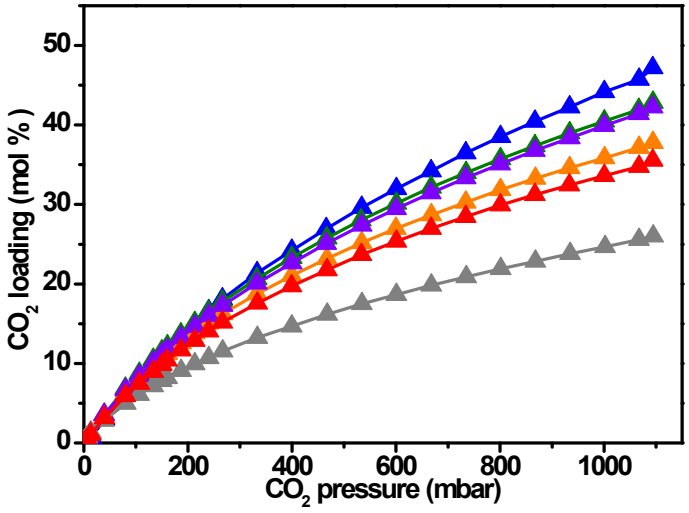

Figure S13. Carbon dioxide adsorption isotherms represented in mol %. of CO_2 respect to the imidazolium at 298 K for samples: **1** (red curve), **2** (blue curve), **3** (green curve), **4** (orange curve), **5** (violet curve), **6** (grey curve). The desorption isotherms are not reported for sake of view.

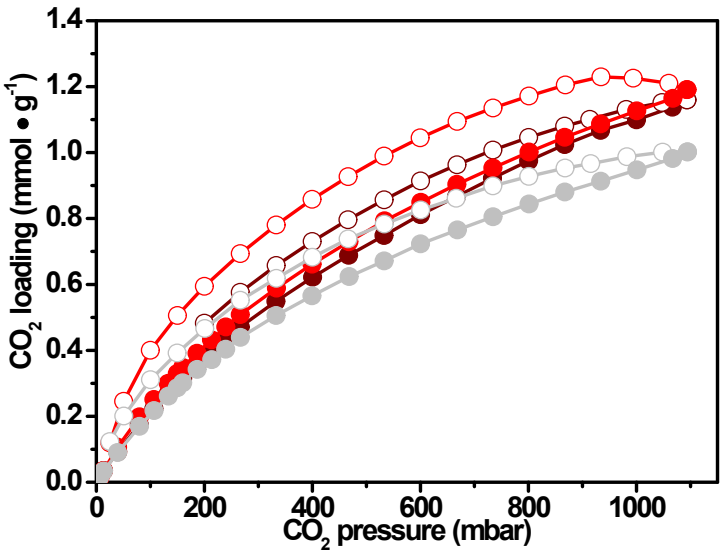

Figure S14. Carbon dioxide adsorption isotherm at 298K for samples: **1** (red curve), **1a** (rusty curve), **1b** (light gray curve). Spheres and circles describe the adsorption branch and the desorption branch respectively.

3.12 Micro-calorimetry

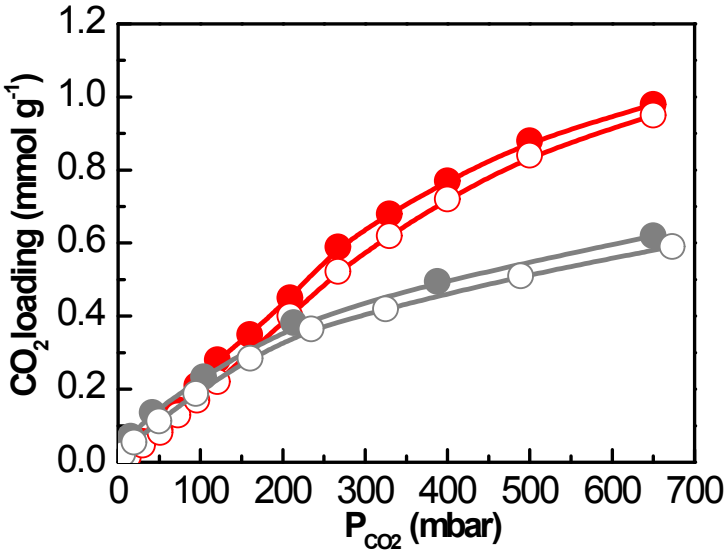

Figure S15. Adsorbed amount as a function of the equilibrium pressure relative to the adsorption at 298 K of CO_2 on samples **1** (red curves) and **6** (grey curves and dots).Spheres refer to the primary adsorption run, whereas circles refer to the secondary adsorption run.

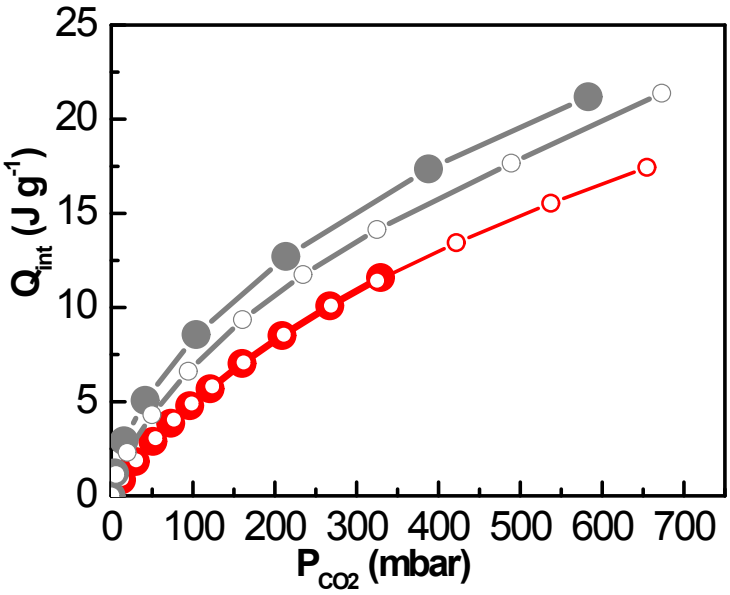

Figure S16. Integrated heat of carbon dioxide adsorption as a function of CO_2 pressure for samples **1** (red curve and dots) and **6** (grey curve and dots). Closed spheres refer to primary adsorption, while open circle refer to secondary one.